Supplemental material

Table of contents

Supplemental Appendix 1. Description of main findings in a case of recurrent C3 glomerulopathy

We present the case of a 47-year-old man (patient GN185) who presents a long history of renal disease since childhood. A chronogram of the disease course is presented in Suppl. Fig. 2A; see Suppl. Appendix 2 for a detailed clinical description. Renal biopsy studies after the third relapse showed membranoproliferative glomerulonephritis, with mesangial hypercellularity, segmental endocapillary hypercellularity, and segmental capillary wall double contours on light microscopy. Immunofluorescence analysis in renal sections showed predominant C3 deposition in the glomerulus in the absence of IgG and, therefore, a diagnosis of C3G was made (Suppl. Fig. 2B).

Quantitative determinations of complement components during the third recurrence demonstrated a slight reduction in plasma C3 levels, otherwise complement components were within the normal range (Suppl. Table 1). Assays to identify C3Nef or anti-FH autoantibodies were negative. Family samples were available from the parents and a sibling, all of them healthy relatives (Suppl. Fig. 3A). Routine Western blot analysis of plasma samples using a polyclonal anti-FH antibody (rb34) that cross-react with FHL-1 and FHR-1 proteins, revealed the presence of two additional bands of approximately 45 kDa in the proband, which were absent in the healthy relatives (data not shown). Additional western blot analysis with a specific monoclonal antibody against FHR-1 also detected the anomalous bands, suggesting an abnormal FHR-1 protein (Suppl. Fig. 3B).

Mutational screening of all complement genes by next generation sequencing did not identify a pathogenic variant in the patient. Copy number variation analysis of the *CFH-CFHR* region by multiple ligation-dependent probe amplification (MLPA) identified a duplication of *CFHR1* exon 3 in the patient sample (Suppl. Fig. 3C). Further characterization of the *CFH-CFHR* loci using a custom-made high density comparative genomic hybridization 15k array, demonstrated the presence of an internal duplication of *CFHR1* exons 2 and 3 in the patient sample (Suppl. Fig. 3D). To identify the break point of this genomic rearrangement, long PCR experiments were performed using a combination of primers to *CFHR1* exon 3 (forward) and intron 1 (reverse), which amplified a DNA fragment only in the patient sample. Further sequencing of such fragment identified the genomic breakpoint within intron 3, where a 10.2 kbp internal duplication containing part of the promoter region and exons 1, 2 and 3 of *CFHR1* is integrated (Suppl. Fig. 3E). This mutant

allele codes for a putative mutant FHR-1 protein that contains a duplication of the dimerization domains SCR1 and SCR2 (Suppl. Fig. 3F). Interestingly, the internal duplication contains 1963 bp of the *CFHR1* promoter region, suggesting that both the mutant and the wild-type FHR-1 protein could be expressed from the same chromosome.

Immunohistochemistry analysis of complement components in the renal tissue of the patient GN185 revealed intense glomerular complement deposition (Suppl. Fig. 4). In addition to the expected C3 staining, C9 was detected within the glomeruli, indicating activation of the complement terminal pathway. C3 staining was mainly due to the presence of the C3 fragments iC3b/C3dg. As expected, glomerular deposition of the FHR-1 protein was also detected using the 2C6 antibody (that recognizes FHR-1, FHR-2 and FHR-5) and a specific mAb against FHR-1 (not shown). In contrast, glomerular FH staining was negative.

Supplemental Appendix 2. Clinical Synopsis of patient GN185

This patient presented a history of recurrent haematuria in association with febrile episodes since 1974, at the age of 6 years. At the age of 10, he developed non-nephrotic proteinuria, a renal biopsy confirmed the diagnosis of membranous glomerulonephritis with sclerosis, and steroid treatment was established during a month. In 1993, at the age of 19, he was admitted to hospital with high blood pressure, renal function impairment [serum creatinine (sCr) 3.4mg/dL] and nephrotic syndrome. He developed end stage renal disease (ESRD) and started hemodialysis in February 1995. He received a kidney transplant from a cadaveric donor in August 1995 and he was treated with prednisone and cyclosporine as immunosuppression (Suppl. Fig. 2A). He had a disease recurrence in October 1996 with nephrotic proteinuria and graft loss 39 months later, starting hemodialysis in 1998. The patient underwent transplantectomy in September 1999, and a histopathologic analysis was performed in the extracted piece. Lesions compatible with membranoproliferative glomerulonephritis type I were found, with the presence of C3 (+++) and IgM (++) by immunofluorescence. He received a second cadaveric transplant in January 2000 and was treated with prednisone, tacrolimus and mycophenolate mofetil. He developed proteinuria in November 2002 and was diagnosed with membranoproliferative glomerulonephritis type I with the presence of C3 (+++) and IgM (+), which lead to the progressive decline of the renal function and graft loss, starting hemodialysis in July 2011. He received a third cadaveric transplant in July 2013 under prednisone, tacrolimus and mycophelonate mofetil as immunosuppression. The graft was functioning since the beginning, showing a progressive improvement in renal function and reaching a sCr of 2mg/dL. In September 2015, he developed nephrotic proteinuria and evidence of glomerular deposition of C3 (+++) and IgM (+) was demonstrated in a new biopsy in November 2015, which in light of the new classification the diagnosis of C3 glomerulopathy was made (Suppl. Fig. 2B). Enalapril treatment was added to the losartan that the patient was already receiving. Complement analysis were undertaken at that time (Suppl. Table 1). The patient received 6 sessions of plasmapheresis after the last relapse (Suppl. Fig. 5A). Since no evidence of renal improvement was observed, eculizumab treatment was initiated at 900 mg/week for the first four weeks and increased to 1200 mg every other week for the following three months. Despite proper C5 inhibition (Suppl. Fig. 5B), proteinuria levels increased, and renal function progressively declined. Hence, eculizumab treatment was interrupted and the patient started in hemodialysis in 2017 (Suppl. Fig. 2A). In September 2020, he received his fourth

cadaveric kidney transplant under prednisone, tacrolimus and mycophelonate mofetil as immunosuppression, and thymoglobulin and a session of plasmapheresis with human immunoglobulin as induction treatment. The graft was functioning since the beginning with progressive improvement of renal function and no proteinuria till the time of this manuscript preparation.

Supplemental Appendix 3. Supplemental Methods

Gene sequencing and copy number variation analysis

Genomic DNA was obtained from peripheral blood mononuclear cells using standard procedures [1]. All complement genes were analyzed by an in-house next generation sequencing panel using the MiSeq next generation sequencing platform (Illumina, USA). Copy number variations in the *CFH-CFHRs* region were assessed by multiple-ligation probe amplification SALSA MLPA P236 A1 ARMD mix 1 kit (MRC Holland, The Netherlands) and in-house designed probe pairs [2]. A custom-designed high-density 8 x 15k oligonucleotide CGH array was used for further characterization of the patient GN185 genomic rearrangement. (Median resolution, 110 bp; AMADID 040193; Agilent Technologies). For the CGH 8 x 15k microarrays, samples were hybridized with sex-matched normal human DNA (Promega Corp.) according to the manufacturer´s instructions. Microarray data were extracted and visualized using Feature Extraction Software (version 10.7) and Genomic Workbench Standard Edition (version 7.0; both Agilent Corp). Copy number-altered regions were detected using ADM-2 (set as 5) statics provided by DNA Analytics, with a minimum number of 5 consecutive probes. Genomic build hg19 was used for the experiment. Microarray data have been deposited in GEO (accession no. GPL16749).

Breakpoint characterization

Long PCR analysis for the characterization of the mutant *CFHR1* allele was designed using a forward primer in *CFHR-1* exon 3 and a battery of reverse primers within *CFHR-1* intron 1. PCR reactions were run in a 1% agarose gel, and a fragment was only amplified in the patient sample when the following pair of primers was used: forward 5´-AAGCGCAGAGATTACCAGAG-3´ and reverse 5´-GGCCCTTGAAATTCGTTTTATT-3´. This amplicon was purified using the NucleoSpin® Gel and PCR Clean-up kit following the manufacturer`s instructions. Subsequently, the fragment was sequenced by Sanger and the results were analyzed in Chromas.

Western blotting

To analyze the FHR-1 native and mutant proteins in the sera of the patient and their relatives, 1 µl of serum was separated in a 12% SDS/PAGE and transferred to PVDF membrane. After blocking with 3% (w/v) bovine serum albumin (BSA) in PBS containing Tween 20 (0.2%), the membrane was hybridized with a mouse anti-FHR-1 primary antibody

(MAB4247, R&D systems) and a goat-anti-mouse secondary antibody labelled with horseradish peroxidase (Cat #31430, DAKO, Denmark). Proteins were detected by using an ECL Western Blotting Substrate Kit (Abcam Inc., Cambridge, MA, USA).

Histologic studies in patient GN185

A tissue sample was collected from the third kidney graft of the patient. The sample was fixed in 3.7 % paraformaldehyde, embedded in paraffin and sectioned at 3 μm. Sections were deparaffinised, hydrated and incubated with 6% goat serum, BSA 4% in PBS for 1h. The following in house primary antibodies were used for staining: 2C6, OX24, 214, MBI6/MBI7, SIM320 12.2.1 and B7 (1:100 dilutions, O/N). In addition, an irrelevant immunoglobulin (Dako) was used at the same concentration in order to assess non-specific staining. Sections were then incubated with anti-mouse biotinylated secondary antibody (1:250 dilution, 1h, Dako) and ABComplex (30 min, Vector lab), followed by staining with 3,30-diaminobenzidine (DAB), hematoxylin counterstaining, and mounting in DPX medium.

Supplemental Table 1: Patient's complement profile during the third relapse.

Component	Patient	Normal range
C3 (mg/dl)	65	70-150
C4 (mg/dl)	26	14-60
FB (µg/ml)	121	85-170
FI (µg/ml)	107	71-115
FH (µg/ml)	135	62-286
FHR-1 (µg/ml)	168	109-153
MCP (%)	102	80-109
C3Nef	Negative	NA
Anti-factor H antibodies	Negative	NA

A

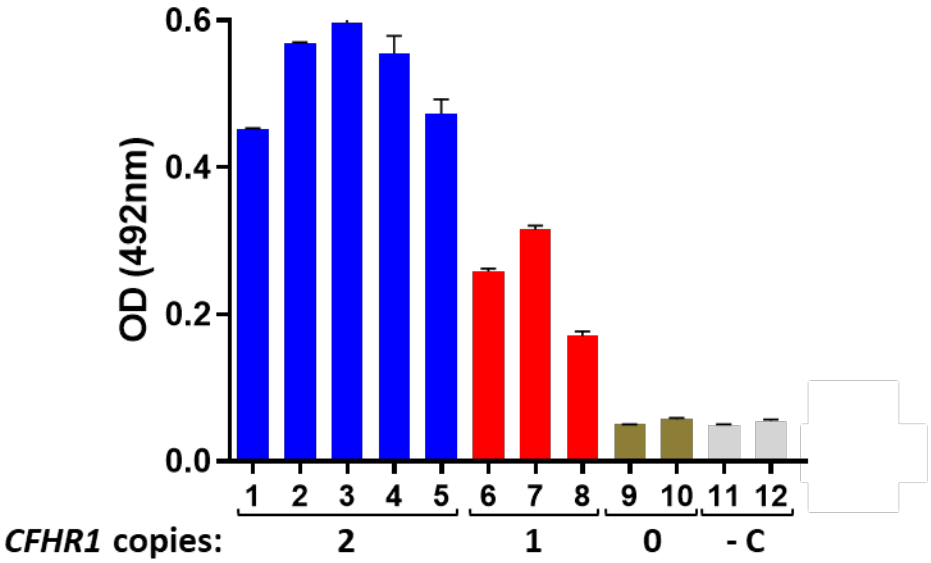

B

Intra-assay CV (N=40)	3,34 %
Inter-assay CV (N=26)	5,44 %

Supplemental Figure 1. Measurement of plasma FHR-1 by sandwich enzyme-linked immunosorbent assay (ELISA). (**A**) Representative ELISA experiment showing the optical density (OD) values obtained at 492nm for the quantification of FHR-1 in plasma samples from individuals carrying either 2, 1 or null copies of the gene encoding FHR-1 (*CFHR1*). PBS containing 1% of BSA was used as a negative control (- c). (**B**) Calculations of intra- and inter-assay coefficient variation (CV) for the FHR-1 ELISA method are depicted in the table. For the intra-assay CV calculation, a total of 40 sample duplicates were analysed. In the case of the inter-assay CV, calculations were based in a sample that was quantified up to 26 different times in independent ELISAs.

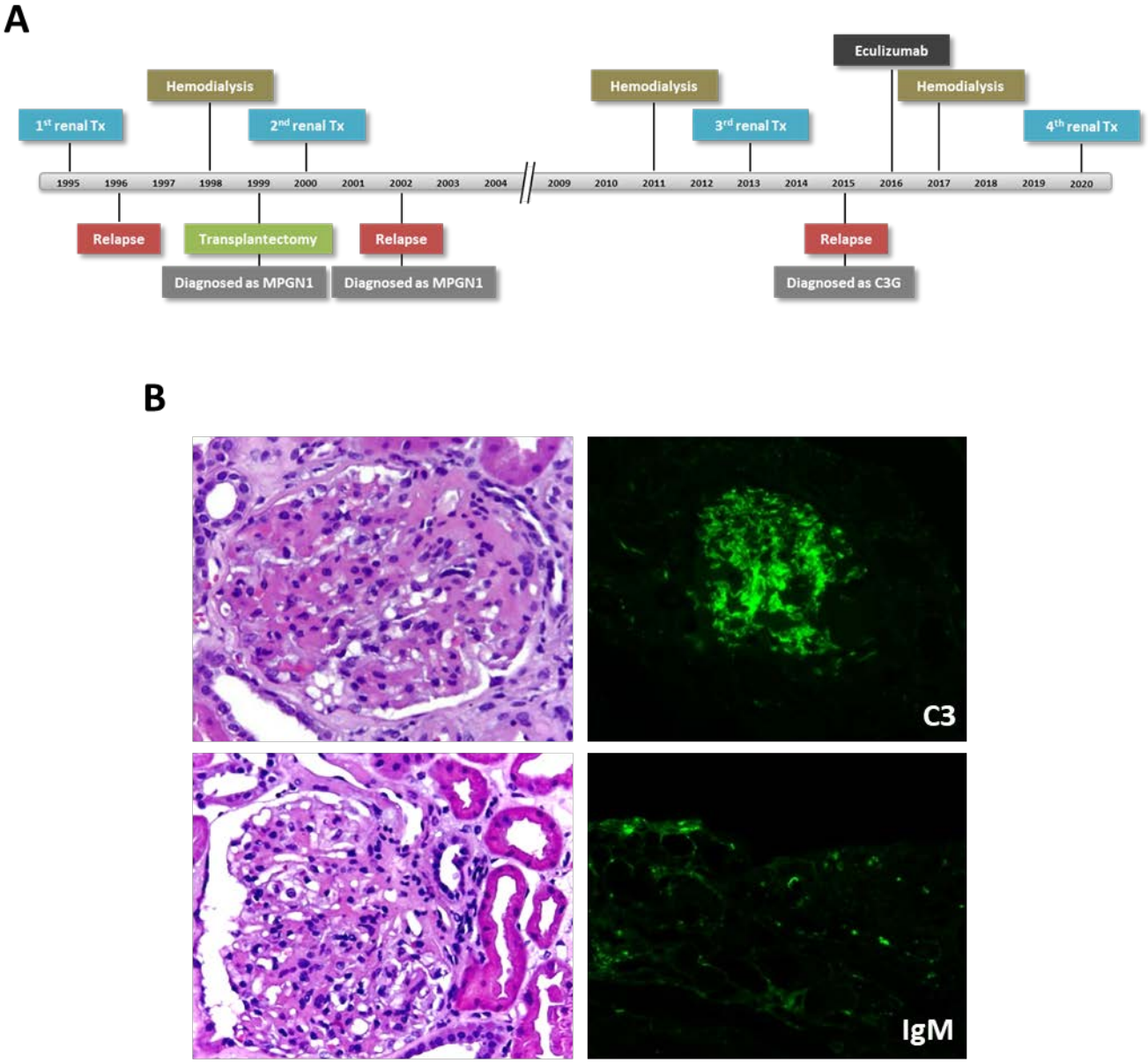

Supplemental Figure 2. Patient´s clinical history and renal histology findings. (**A**) The timeline for the four kidney transplants, relapses, disease diagnosis and main therapeutic interventions of the patient is shown. (**B**) Renal biopsy investigations performed after the relapse in 2015. Light microscopy showing a periodic acid–Schiff–stained glomerulus and immunofluorescence of C3 and IgM in the patient renal tissue.

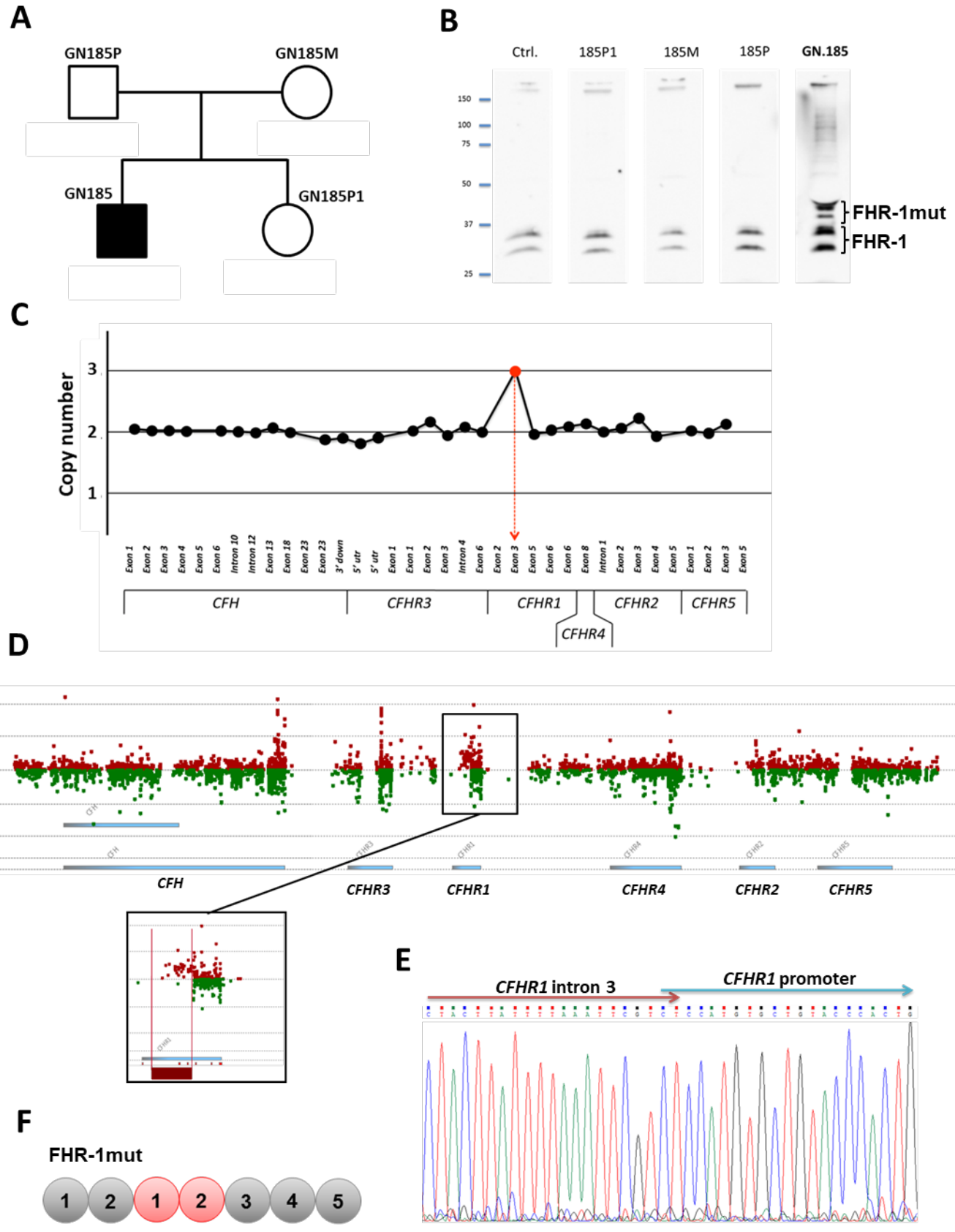
A
GN185P
GN185M
GN185
GN185P1
B
Ctrl.
185P1
185M
185P
GN.185
150
100
75
50
37
25
FHR-1mut
FHR-1
C
Copy number
3
2
1
Exon 1 Exon 2 Exon 3 Exon 4 Exon 5 Exon 6 Intron 10 Intron 12 Exon 13 Exon 18 Exon 23 Exon 23 3' down 5' utr 5' utr Exon 1 Exon 1 Exon 2 Exon 3 Intron 4 Exon 6 Exon 2 Exon 3 Exon 5 Exon 6 Exon 6 Exon 8 Intron 1 Exon 2 Exon 3 Exon 4 Exon 5 Exon 1 Exon 2 Exon 3 Exon 5
CFH
CFHR3
CFHR1
CFHR2
CFHR5
CFHR4
D
CFH
CFHR3
CFHR1
CFHR4
CFHR2
CFHR5
E
CFHR1 intron 3
CFHR1 promoter
F
FHR-1mut
1
2
1
2
3
4
5

Supplemental Figure 3. An internal duplication in *CFHR1* segregates with C3G in pedigree GN185. (**A**) The pedigree of GN185. (**B**) Western blot analysis of FHR-1 in plasma samples from pedigree GN185 using a monoclonal anti-FHR-1 antibody. Apart from the bands corresponding to the wild-type FHR-1, anomalous bands were only detected in the patient's sample. (**C**) A duplication of a probe within *CFHR1* exon 3 (red dot) was detected by multiplex ligation-dependent probe amplification analysis compared with a control sample. (**D**) High resolution CGH array of the *CFH-CFHRs* locus demonstrates an internal duplication involving at least exons 2 and 3 in the genomic DNA from GN185. (**E**) Chromatogram of the corresponding DNA sequence surrounding the genomic breakpoint in mutant *CFHR1* reveals that the breakpoint occurs at position IVS3+1004 (in the first intron 3 of the duplicated *CFHR1*) and c.1-1963 (counting from the second exon 1 of the duplicated *CFHR1*). (**F**) Schematic of the 7 SCR structure of the putative protein expressed by the mutant *CFHR1* allele. Duplicated SCR domains 1 and 2 are denoted in red.

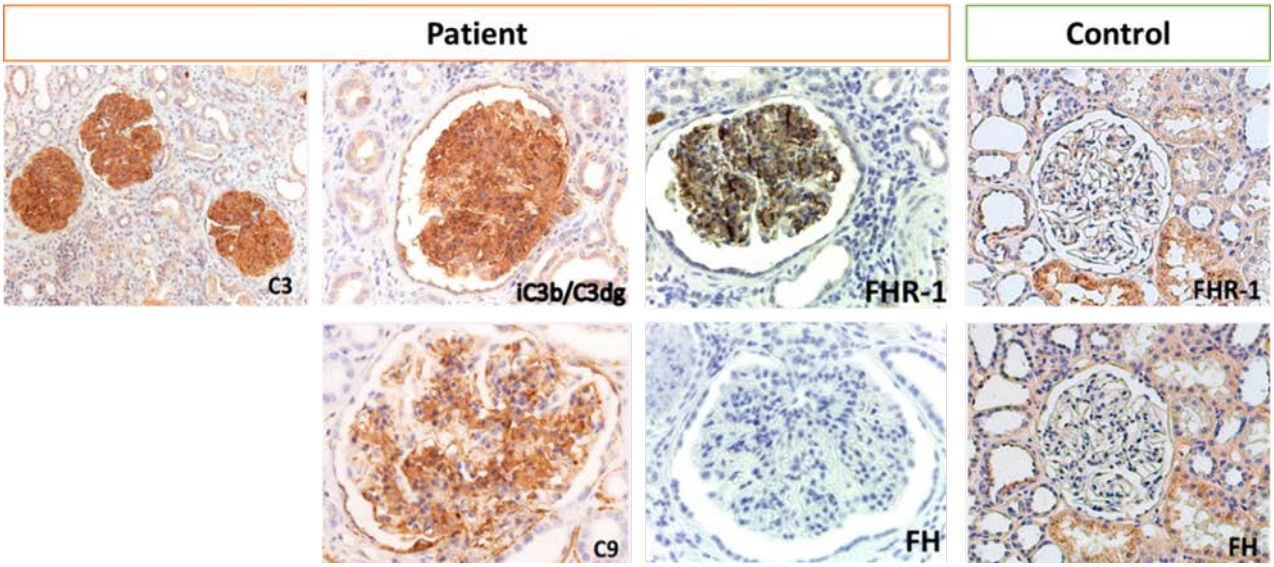

Supplemental Figure 4. Immunohistochemistry of complement components in the patient's renal tissue. Immunohistochemistry of C3, iC3b/C3dg, C9, FHR-1 and FH performed on the renal biopsy of patient GN185 demonstrated strong glomerular deposition of all analysed components but FH. FHR-1 and FH immunohistochemistry on a control renal tissue is also shown.

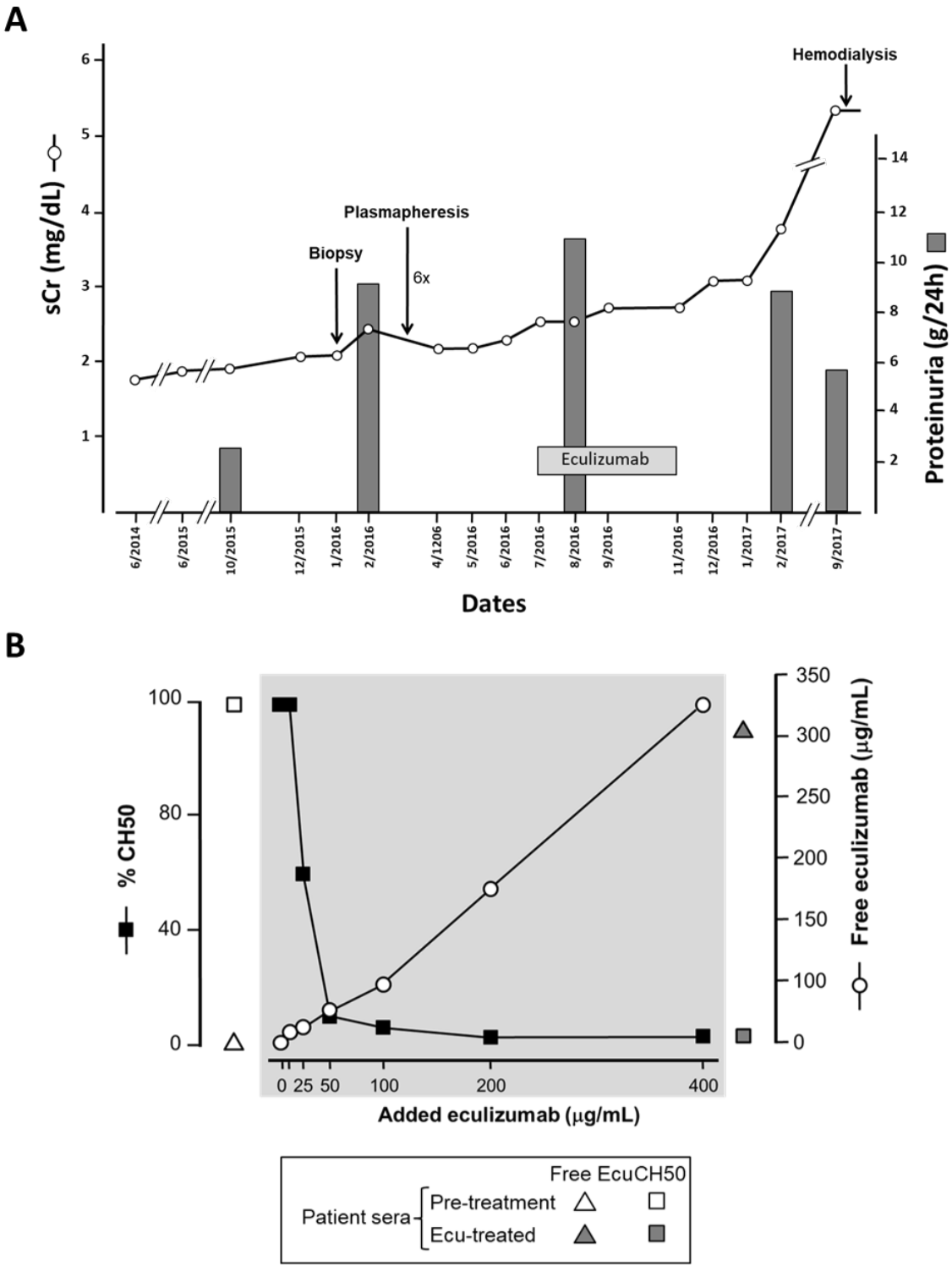

Supplemental Figure 5. Patient's renal function evolution and treatments and evaluation of C5 inhibition by eculizumab. Serum creatinine (sCr), proteinuria and major therapeutic interventions are depicted for the patient's last 6 years (**A**). The ability of eculizumab to inhibit C5 activation in the patient's serum was evaluated in CH50 hemolytic assays (black squares) and by ELISAs measurement of free eculizumab (open circles) (**B**).

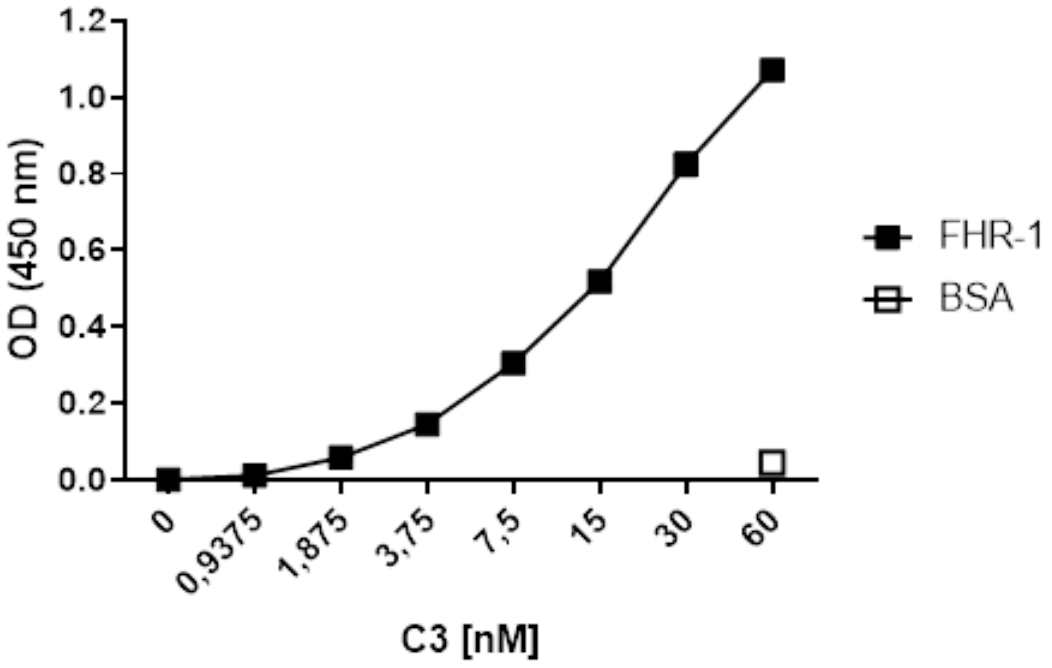

Supplemental Figure 6. Binding of C3 to surface-bound FHR-1. FHR-1 (150 nM) diluted in PBS was immobilized in a microtiter plate O/N at 4ºC. After blocking with 1% BSA in Tris-Tween, serial dilutions (0.93-60nM) of C3 (Complement Technologies, Tyler, TX, USA) were incubated for 1h at RT. PBS containing BSA (60 nM) was used as a negative control. After extensive washing, the bound C3 was detected using the monoclonal mouse anti-human C3 12.17 antibody[3] and a HRP-conjugated goat anti-mouse IgG as secondary antibody (Dako, Cat. Num. 31430). A representative experiment of a total of three independent experiments is shown. Mean values and standard deviations are depicted.

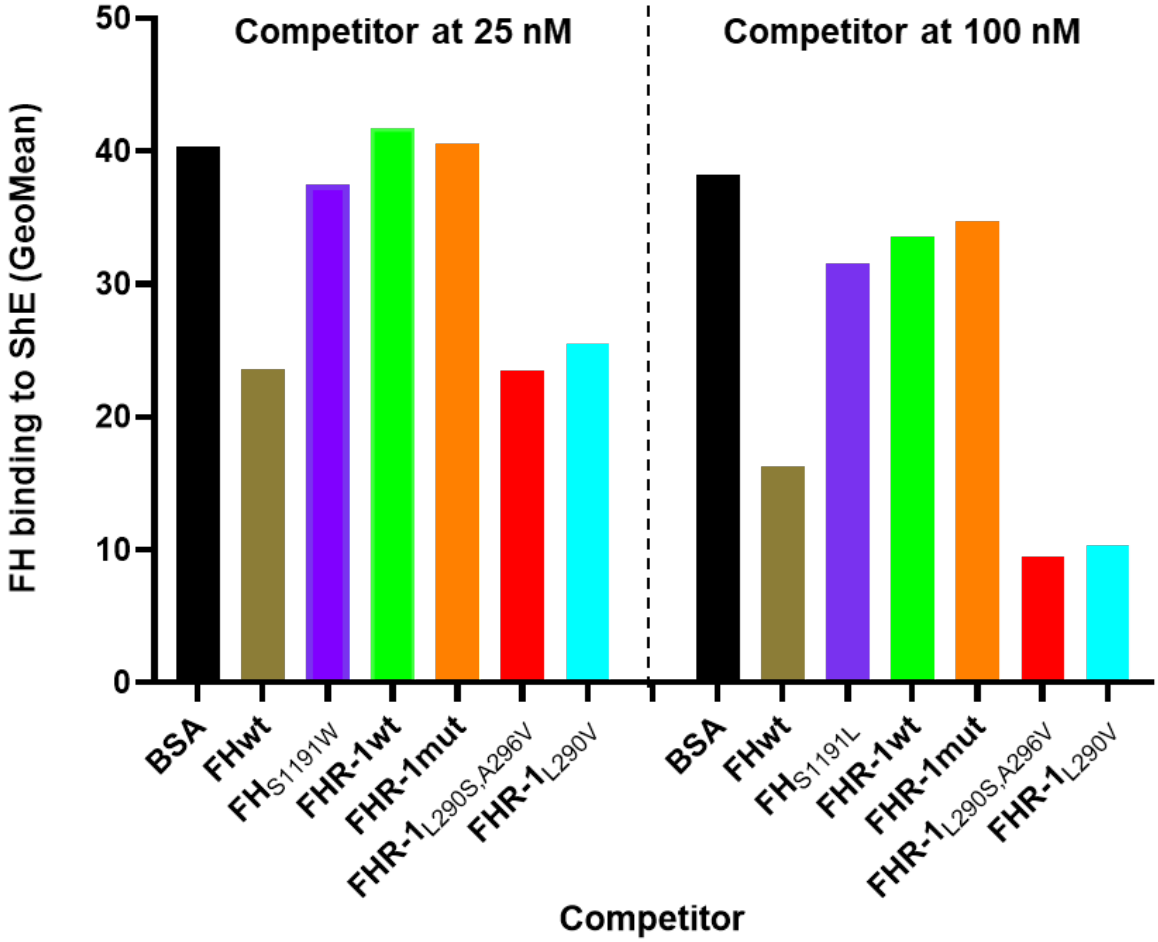

Supplemental Figure 7. FH C3b binding competition assay in sheep erythrocytes (ShE). The binding of 50 nM FH labelled with alexa fluor 488 (FH^{AF488}) to opsonized ShE (C3-ShE) was assayed in the presence of either 25 nM or 100 nM amounts of wild-type FH (FHwt), FHR-1wt, FHR-1mut, and the aHUS-associated mutant proteins $FHR\text{-}1_{L290S,A296V}$ and $FHR\text{-}1_{L290V}$ that, like FH, have the ability to bind sialic acid [4,5] and FH_{S1191W}, an aHUS-associated mutant protein that loses the capacity to bind sialic acids . Equivalent amounts of BSA (50 or 200 nM) were used as a negative control and, hence, represent the binding of FH^{AF488} to the C3-ShE when the molecule is not competed. The binding of FH^{AF488} was analysed by flow cytometry and the obtained geometric mean (GeoMean) is represented. Neither FHR-1wt, FHR-1mut nor FH_{S1191W} compete FH^{AF488} binding to the cells. Only the aHUS associated FHR-1 mutant proteins and FHwt displace the FH^{AF488} from binding the C3-ShE at the tested concentrations.

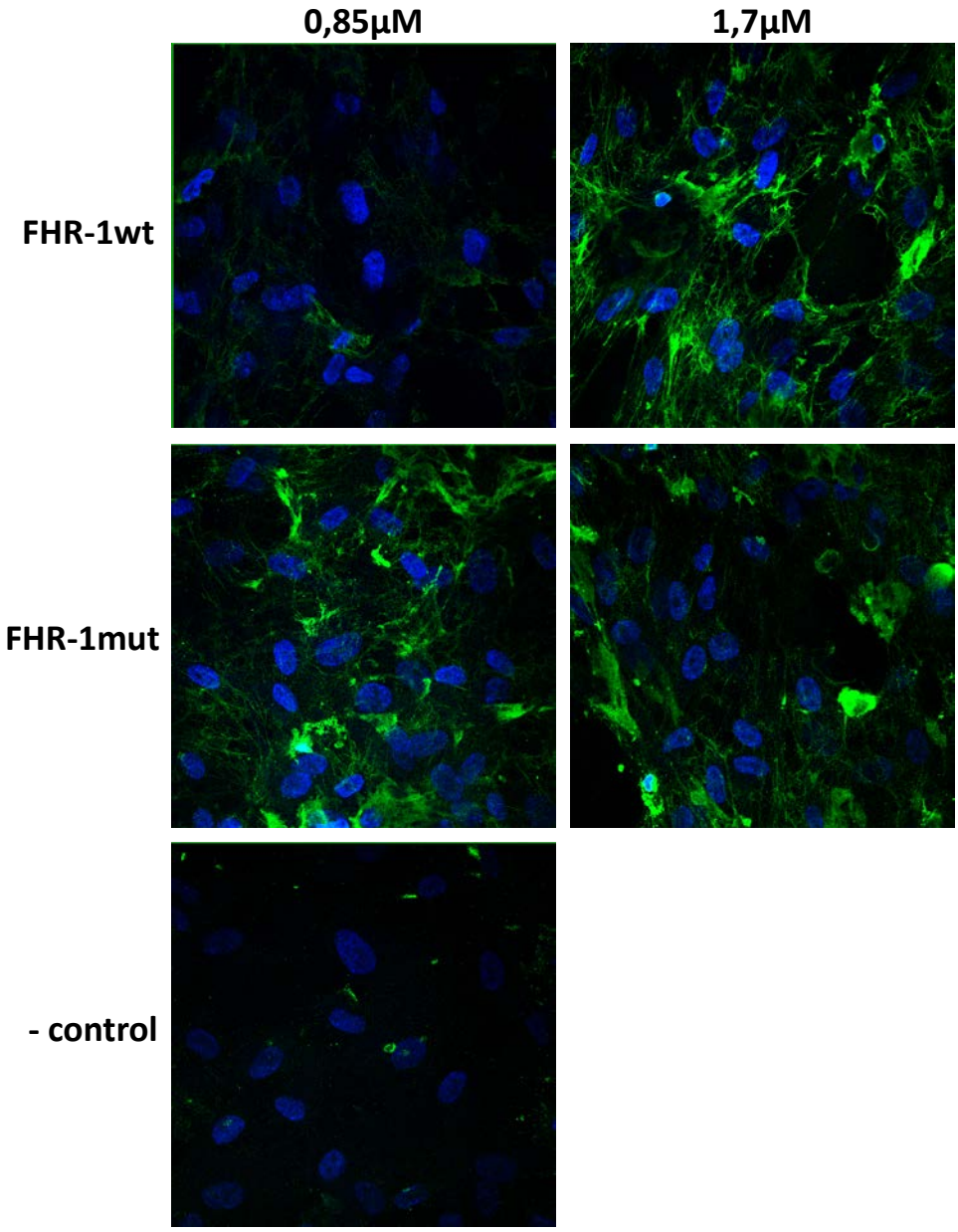

Supplemental Figure 8. FHR-1 binding to human renal epithelial (HREpi) cells. Purified recombinant wild-type and mutant FHR-1 proteins were incubated at 0.85 and 1.7 µM with HREpi cells, and protein binding was detected with the 2C6 antibody. In this setting, the mutant FHR-1 protein bound more efficiently than the wild-type protein. In the negative control no FHR-1 proteins were added prior to the antibodies.

A

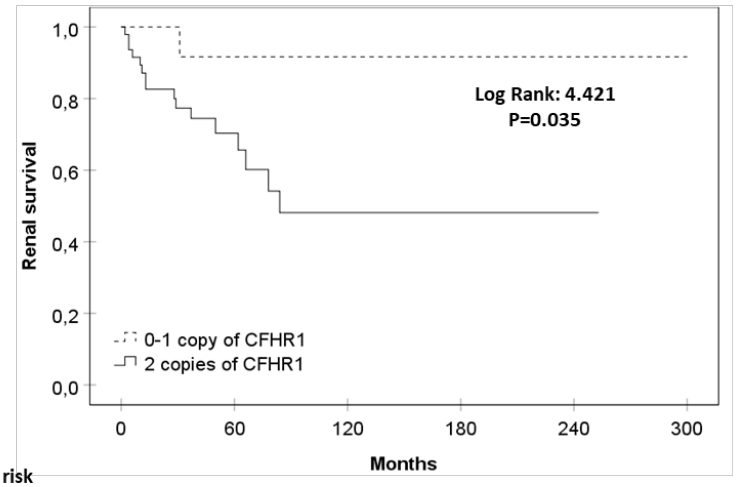

Patients at risk						
0 or 1 copy of *CFHR1*	16	15	15	15	15	15
2 copies of *CFHR1*	48	36	32	32	32	-

B

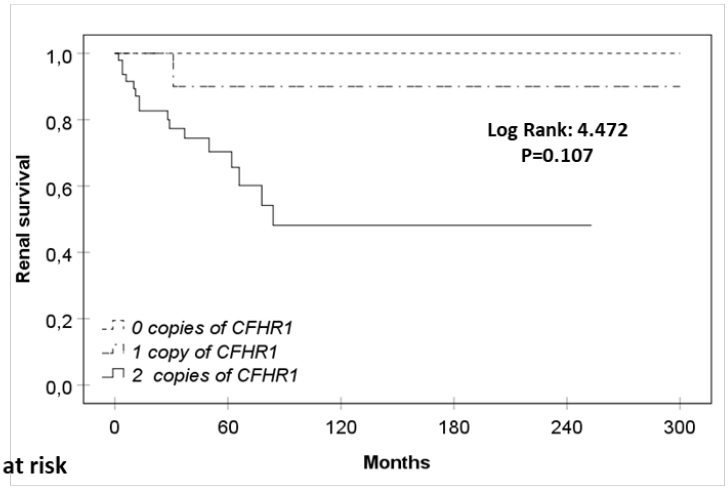

Patients at risk						
0 copies of *CFHR1*	4	4	4	4	4	4
1 copy of *CFHR1*	12	11	11	11	11	11
2 copies of *CFHR1*	48	36	32	32	32	-

Supplemental Figure 9. Kaplan-Meier curves for kidney survival according to the presence of *CFHR1* copy number in patients without complement pathogenic variants. End-stage renal disease (ESRD) was considered as the event and a follow-up of 300 months is depicted. (**A**) Kidney survival rate was compared between patients with 0 or 1 copy of *CFHR1* and patients with 2 copies of the gene. In this case, lower *CFHR1* copy number was significantly associated with better renal survival. (**B**) Stratification of the patients in three groups according to the presence of 0, 1 or 2 copies of *CFHR1*, confirms that the lower *CFHR1* copy number the better kidney survival rate, although the difference is not statistically significant due to the low number of patients in each group.

Supplemental Appendix 4. References

1. Miller SA, Dykes DD, Polesky HF. A simple salting out procedure for extracting DNA from human nucleated cells. *Nucleic Acids Res.* Feb 11 1988;16(3):1215.

2. Abarrategui-Garrido C, Martinez-Barricarte R, Lopez-Trascasa M, de Cordoba SR, Sanchez-Corral P. Characterization of complement factor H-related (CFHR) proteins in plasma reveals novel genetic variations of CFHR1 associated with atypical hemolytic uremic syndrome. *Blood.* Nov 5 2009;114(19):4261-4271.

3. Subias Hidalgo M, Yebenes H, Rodriguez-Gallego C, et al. Functional and structural characterization of four mouse monoclonal antibodies to complement C3 with potential therapeutic and diagnostic applications. *Eur J Immunol.* Mar 2017;47(3):504-515.

4. Dopler A, Stibitzky S, Hevey R, et al. Deregulation of Factor H by Factor H-Related Protein 1 Depends on Sialylation of Host Surfaces. *Front Immunol.* 2021;12:615748.

5. Martin Merinero H, Subias M, Pereda A, et al. The molecular bases for the association of FHR-1 with atypical hemolytic uremic syndrome and other diseases. *Blood.* Mar 2 2021.